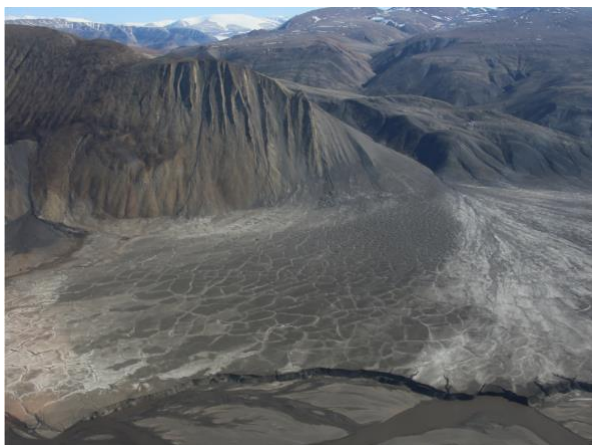


**3D-MODELLING OF SUBSURFACE ICE USING GROUND PENETRATING RADAR ON AXEL HEIBERG ISLAND, CANADIAN HIGH ARCTIC.** C. N. Andres<sup>1</sup>, G. R. Osinski<sup>1</sup>, and E. Godin<sup>2</sup>. <sup>1</sup>Department of Earth Sciences/Institute for Earth and Space Exploration, University of Western Ontario, London, ON, Canada, N6A 5B7, candres5@uwo.ca, <sup>2</sup>Centre d'Études Nordiques, Université Laval, Québec, QC, Canada, G1V 0A6.

**Introduction:** Ground penetrating radar (GPR) is a geophysical technique that allows high-resolution and non-destructive stratigraphic imaging of the subsurface. The GPR method records the two-way travel time of electromagnetic (EM) waves reflected at boundaries between subsurface layers with contrasting relative permittivity. Dielectric contrasts develop due to variations in sediment grain size, water content, and mineral composition.

The overall objective of this research is to survey an area of Axel Heiberg Island, Nunavut, to identify and map near-surface ice and other structural features beneath the ground. This will be used to correlate potential similar scale geomorphologic features on Mars. Comparatively, theoretical models indicate that water ice is stable in the shallow subsurface (depths of <1–2 m) of Mars at high latitudes [1,2]. Landsystem analysis techniques are also used to investigate different components of the periglacial landscape (i.e. gullies, polygons) to better inform our understanding of the formation/interaction of these features on Mars.

**Study Site:** Using an Earth analogue site similar to environments on Mars, the GPR survey was conducted on an alluvial “fossil” fan deposit from a mass wasting event. Due to the relative inactivity of this fan, it has been overprinted with polygonized terrain as well as dominated by periglacial processes of repeated freezing and thawing (**Figure 1**). The region of interest is located in Strand Fjord, Axel Heiberg (79°09'43"N, 90°13'44"W) that shows different tonalities of the “fossil” fan due to the past flow of water in this region.



**Figure 1.** A polygonized “fossil” fan on Strand Fjord, Axel Heiberg Island. The high albedo or light colour-toned features on the fan are water-marker indicators of mineral deposits (i.e. gypsum). There is a smaller, more recently active fan to the left-most of the image.

At the present day, Strand Fjord is dominated by periglacial landscape processes (i.e. freeze-thaw, cryogenic cooling, etc.). However, upon its formation, the region was volcanically active in the Late Cretaceous (~100.5 Ma) as part of the Sverdrup Basin succession. Strand Fjord volcanics are encased with a maximum thickness of ~789 m on the northwestern part of Axel Heiberg mainly composed of volcanoclastic conglomerates, sandstones, mudstones, and coal deposits [3].

**Methods:** For this procedure, a 25 m x 25 m grid was set up, while following the “zamboni” method making a zigzag pattern with a step-size of 1 m intervals. 25 lines were oriented north-south and 25 lines were oriented in the west-east direction. This resulted in a total of 50 radar files and a total of ~180 time slices from the interpolated GPR map (**Figure 2**). The equipment used in the survey is the Sensors and Software 250 MHz Noggin GPR with a 0.4 m to 3 m penetration depth. Additionally, a series of calibration tests were done to ensure the least signal deviation.

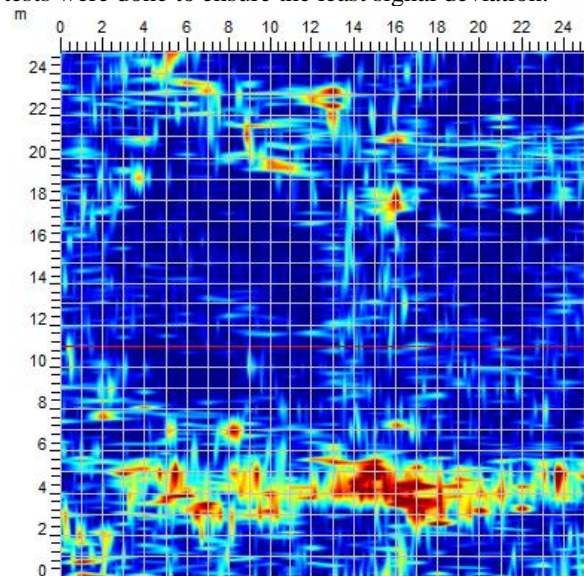


**Figure 2.** Time slice at depth  $z = 0.8$  m highlighting ice-rich features in red/green that are widely concentrated at polygon troughs ( $x = 15$  m,  $y = 4$  m). There are a total of 5 polygons covered by the survey grid as seen from the shape of the signal returns.

**Results:** Data collected from this survey was interpreted via extrapolation/calculation of conductivity, permittivity, travel-time velocity, penetration depth, and radar reflection coefficient (RC) using the EKKO\_Project software along with topographic data.

The goal of the GPR reflection survey is to determine valuable amplitude traces that can potentially be mapped to locate the position/saturation of ice-wedges in the subsurface and to distinguish probable stratigraphic boundaries in frozen ground.

**GPR Radargram Profiles.** There were a total of 50 radargrams produced by the survey. By calibrating radargrams to extract velocity information, the calibrated velocity of the survey was found to be 0.064 m/ns, which indicates a wet clay/sand subsurface. This extracted velocity can then be used for further analysis and more accurate stratigraphic observations thereby making plausible interpretations (**Figure 3**). In the radargram, there are various subsurface features that can be seen as summarized in **Table 1**.

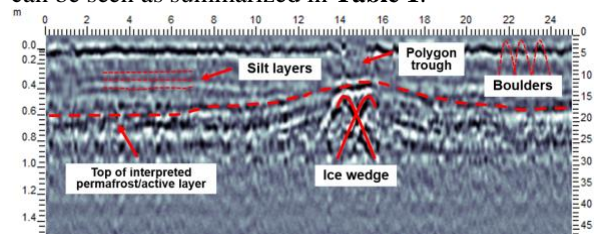


**Figure 3.** Stratigraphic cross-section of one GPR line along a polygon center-trough-center showing features such as, ice at  $x = 15$  m and  $z = 0.8$  m (depth of ice).

**Table 1.** Sub-surface features as seen on radargram responses using the Noggin 250 MHz GPR in Figure 3.

Depth (z)	Feature
0.0 m – 0.4 m	polygon trough
0.3 m – 0.5 m	layering of silt/sand horizons
0.6 m	top of the active layer (frozen ground)
0.8 m	ice-wedge
>1.0 m	signal attenuation due to the poor GPR response from the thawing of permafrost

**GPR-derived 3D Model.** In order to model GPR data, an isosurface needs to be created in order to illustrate 3D shaded renderings from lattice files. They reflect the concept of a contour line (2D) and frames it in 3D space using matrices. Isosurfaces also display constant data values for a component that dissects a 3D volume, which in this case are the highest returns (filtered for ice-rich GPR signals).

Using the Voxler 4 software, a 3D simulation of ice-wedges can be modelled not only as a visualization tool but also as a calculator for subsurface ice volume (**Figure 4**). Volume calculations are generated from voxels (3D pixels) that are either partially or fully included in the isosurface. The total volume (isovalue) is the sum of the individual volumes from these voxels. Using this approach, the volume of the ice-rich isosurface within the 25 m x 25 m GPR survey grid has been calculated to contain 43.28 m<sup>3</sup> of ice.

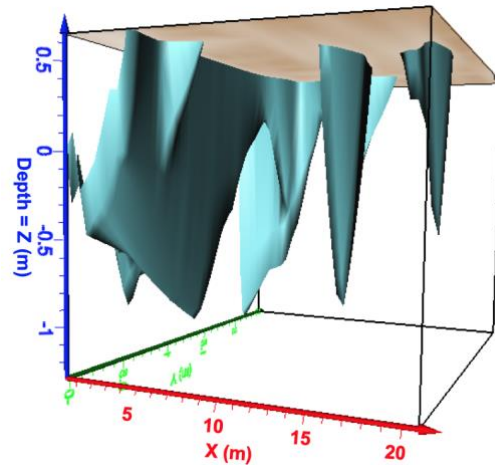


**Figure 4.** A snapshot of a 3D lattice video simulation, showing ice-wedge geometry and volume in cyan. The bounding box corresponds to dimensions in Figure 2, with the ice-wedge in Figure 3 mapped at  $x = 15$  m.

**Discussion:** Previous work has been able to approximate the amount of ice from GPR depth slices without isolating the ice [4, 5]. However, 3D modelling of GPR data can be limited by several factors, two of which are near-surface water and mineral concentration. Due to the soil's conductive nature, the GPR signals get “scattered” before it can return to the antenna when travelling through damp or wet soils, especially when they have high salt content. GPR data is a crucial tool to validate cored-and-cached samples that may be indicative of paleoenvironments. To validate this GPR model, a 12m sedimentological log of the “fossil” fan along with 9 sediment pits were also dug/recorded in order to ground-truth features that we’re seen on the scan. The sedimentological column strongly validates the depth of the active layer at  $z = 0.6$  m and the ice-wedge at  $z = 0.8$  m. This was repeated for other GPR cross-sections with accurate correlations.

**Future Work:** Although this work is currently being done on subsurface ice on polar desserts on Earth as a reference point, subsurface ice on Mars also exists in regions that are highly dominated by periglacial regimes. Moreover, it is important to expand on the broad capabilities of subsurface radar imaging as it is a powerful tool in seeing the invisible especially when supplemented by analysis of soil, mineral composition, and remote sensing. 3D GPR offers considerable potential for imaging, interpreting, and 3D mapping of near-surface ice in periglacial environments.

**References:** [1] Bandfield, J.L. (2007). *Nature*, 447(7140), p.64. [2] Levy, J. et al. (2009). *JGR: Planets*, 114(E1). [3] Ricketts, B. et al. (1985). *Polar Research* 3, no. 1: 107-122. [4] Munroe, J.S. et al. (2007). *Permafrost and Periglacial Processes*, 18(4), pp.309-321. [5] Stuurman, C.M. et al. (2016). *Geophysical Research Letters*, 43(18), pp.9484-9491.